



Fermi National Accelerator Laboratory

TM-1694

Main Ring Transition Crossing Simulations *

Ioanis Kourbanis and King-Yuen Ng
Fermi National Accelerator Laboratory
P.O. Box 500
Batavia, Illinois 60510

October 1990

* Submitted to the proceedings of the Fermilab III Instabilities Workshop, St. Charles, Illinois, June 25-29, 1990.



Operated by Universities Research Association Inc. under contract with the United States Department of Energy

MAIN RING TRANSITION CROSSING SIMULATIONS

Ioanis Kourbanis and King-Yuen Ng

Fermi National Accelerator Laboratory, P.O. Box 500, Batavia, IL 60510*

I. INTRODUCTION

We used ESME¹ to simulate transition crossing in the Main Ring (MR). For the simulations, we followed the MR 29 cycle used currently for \bar{p} production with a flat top of 120 GeV. In Sect. II, some inputs are discussed. In Sect. III, we present simulations with space charge turned off so that the effect of nonlinearity can be studied independently. When space charge is turned on in Sect. IV, we are faced with the problem of statistical errors due to binning, an analysis of which is given in the Appendices. Finally in Sects. V and VI, the results of simulations with space charge are presented and compared with the experimental measurements.

II. SOME INPUTS

1. Rf voltage and acceleration

The typical rf high voltage curve in Fig. 1 was reproduced as accurately as possible by breaking it down into many segments. The rf phase was chosen automatically by following the acceleration curve in Fig. 1.

2. Initial bunch area and number per bunch

Since the longitudinal emittance (bunch area) at injection in the MR depends strongly on the intensity of the beam, i.e., the number of booster-turn injection from the linac, actual measurements were made and the results are compiled in Table I. The numbers in this table were used as input to ESME for the initial bunch emittance and the number of particles per bunch in order to simulate the performance of the MR as closely as possible.

*Operated by the Universities Research Association, Inc., under contract with the U.S. Department of Energy.

| No. of Booster Turns | Bunch Area ϵ_L (eV-s) | No. Particle per Bunch ($\times 10^{10}$) |
|-------------------------|-----------------------------------|--|
| 2 | 0.09 | 0.9 |
| 3 | 0.10 | 1.3 |
| 4 | 0.12 | 1.6 |
| 5 | 0.16 | 1.8 |

Table I: Bunch area and number per bunch for different booster cycles.

3. Nonlinear phase-slip

The phase-slip parameter η is defined as

$$\eta = \alpha_p - \frac{1}{\gamma^2}, \quad (2.1)$$

where the momentum compaction factor α_p is not a constant. At momentum p , it can be expanded about the synchronous momentum p_0 as

$$\alpha_p(p) = \alpha_0^{\#} + \alpha_1^{\#} \delta + \alpha_2^{\#} \delta^2 + \dots, \quad (2.2)$$

where

$$\delta = \frac{p - p_0}{p_0}. \quad (2.3)$$

Here,

$$\gamma_T = \frac{1}{\sqrt{\alpha_0}} \quad (2.4)$$

is the transition gamma of the synchronous particle, and $\alpha_i^{\#}$ with $i = 1, 2, \dots$ are called the nonlinear coefficients of the momentum compaction factor. In these simulations, only the lowest nonlinear coefficient $\alpha_1^{\#}$ is included. The $\alpha_i^{\#}$ defined in Eq. (2.2) (the same in ESME) are different from the nonlinear coefficients α_i^J in the power-series expansion of orbit length defined originally by Johnsen.² In fact, the lowest- and first-order coefficients[†] are related by

$$\alpha_0^{\#} = \alpha_0^J \equiv \alpha_0,$$

[†] Actually α_1^J is called α_2 in Johnsen's paper.

$$\alpha_1^{\mathcal{B}} = \alpha_0(1 + 2\alpha_1^{\mathcal{J}} - \alpha_0) . \quad (2.5)$$

Without turning on any sextupoles to correct for the natural chromaticity, $\alpha_1^{\mathcal{J}} \approx 1$. For the MR, $\alpha_0 = 0.002844$ corresponding to $\gamma_T = 18.75$. In the actual MR 29 cycle, natural chromaticity is mostly corrected and $\alpha_1^{\mathcal{J}} \approx 0$. Thus $\alpha_1^{\mathcal{B}} \approx \alpha_0$. In our simulations, we took $\alpha_1^{\mathcal{B}} = 3.0 \times 10^{-3}$.

4. Space charge

The longitudinal space charge can be included in ESME by a longitudinal space-charge impedance

$$\frac{Z_{sc}}{n} = i \frac{Z_0 g}{2\beta\gamma^2} , \quad (2.6)$$

where $Z_0 = 377 \Omega$ is the free-space impedance and the geometric factor g is

$$g = 1 + 2 \ln \frac{b}{a} \quad (2.7)$$

with b and a denoting, respectively, the radius of the beam pipe and the radius of the beam. In the simulations with space charge, $g = 6.5$ was used.

The transverse space-charge force will lower the betatron tune and therefore the transition γ of those particles near the axial center of the bunch by a larger amount than those particles at the transverse edge. Thus, particles near the center will cross transition at an earlier time than those at the edge. This effect, known as the Umstätter's effect,³ is very similar to the Johnsen's nonlinear effect,² with the exception that it is intensity dependent. Following the estimation performed in Ref. 4, assuming a transverse beam half-width and half-height of 5 mm, a γ_T depression of $\Delta\gamma_T \sim 0.025$ is obtained. With $\dot{\gamma} \sim 100/\text{sec}$, some particles at the center of the bunch will cross transition at a time $\Delta T = \Delta\gamma_T/\dot{\gamma}_T \sim 0.25$ ms earlier. Since this time is much less than the nonadiabatic time $T_c = 2.97$ ms for the MR and Umstätter's effect is not presently incorporated in ESME, transverse space charge has not been included in our simulations.

III. SIMULATIONS WITHOUT SPACE CHARGE

The simulation of the MR 29 cycle was first performed with space charge turned off and with $\alpha_1^{\mathcal{B}} = 3.0 \times 10^{-3}$. No other impedances were imposed. The effect of

transition crossing is therefore intensity independent and only the effect of nonlinearity is important. By nonlinearity, we mean a nonzero dynamic nonlinear coefficient α_1^f and a nonzero (actually 1.5) kinematic coefficient in Eq. (3.1) below, which imply that particles with different momenta cross transition at different times. The spread in crossing time is called the *nonlinear time*,⁵ and is defined as

$$T_{\text{NL}} = \left(\alpha_1^f + \frac{3}{2} - \frac{\alpha_0}{2} \right) \frac{\gamma_T}{\dot{\gamma}_T} \frac{\Delta p}{p_0}, \quad (3.1)$$

where $\dot{\gamma}_T$ is the rate of change of γ at transition and $\Delta p/p_0$ is the fractional half-spread of momentum.

We performed the simulations with five thousand macro-particles per bunch at different initial bunch emittances. No particle loss was observed across transition when the initial bunch emittance was below $\epsilon_L = 0.18$ eV-sec, which corresponded to 5 booster-turn injection. We started to see a loss of 1.5% when the initial bunch emittance reached $\epsilon_L = 0.24$ eV-sec. The growth in bunch area as a function of initial bunch emittance is shown in Fig. 2(a) and the particle loss at transition as a function of initial emittance is shown in Fig. 2(b). For pure nonlinear effect,⁶ the fractional increase in bunch emittance is proportional to the square root of the initial bunch emittance, or

$$\frac{\Delta \epsilon_L}{\epsilon_L} \propto \sqrt{\epsilon_L}. \quad (3.2)$$

We see that the results in Fig. 2(a) agree with such a dependency. We also see from Fig. 2(b) that the number of particles lost across transition increases rapidly with the initial bunch emittance. This is a typical consequence of the nonlinear effect, because a bigger ϵ_L implies a larger momentum spread in the beam and therefore a bigger nonlinear time.

IV. PROBLEMS ASSOCIATED WITH SPACE-CHARGE SIMULATION

The actual performance of the MR was simulated. As a result, the emittance and particles per bunch in Table I was followed with space charge turned on.

The first thing observed was a blowup of bunch emittance and a loss of particles even before transition. For example, for 5 booster-turn injection, the bunch emittance

grew by a factor of about three from 0.164 eV-sec to 0.483 eV-sec as shown in Fig. 3(a), accompanied by a particle loss of 7.7% before transition in the simulation as shown in Fig. 3(b). The total particle loss was 20.5%. However, the bunch emittance did not grow further across transition, in contradiction to Eq. (3.2) if nonlinearity were the dominating effect. Closer study of the simulation revealed that the growth had been limited by the bucket area which shrunk to a minimum of 0.49 eV-sec only after transition. As a result, we saw a big particle loss instead. Note that bucket area is the actual area of the bucket, whereas bunch emittance is defined here as 6π multiplied by the product of the rms bunch length and rms energy spread of the bunch. In this simulation, $N_t = 2000$ macro-particles were tracked, $N_b = 512$ bins were used for a rf wavelength, and $\alpha_1^p = 1.0 \times 10^{-3}$ was assumed.

The growth of bunch area and particle loss before transition were in fact unphysical. There are two possible reasons for this artifact. They are the unmatched bunch shape and the incorrect binning.

1. Unmatched bunch shape

In ESME, we populate a bunch according to a certain form of distribution and a certain bunch emittance to fit the rf bucket *without* the consideration of space charge. As space charge is turned on in the tracking, the rf potential will be altered. The initial bunch will no longer fit the space-charge modified bucket. It tumbles inside the bucket and results in a growth of bunch emittance. If the bunch is big enough to start with, the space-charge loaded bucket may not be big enough to hold it, and particle loss will occur.

There have been many different proposals and ideas of how to eliminate these artificial effects due to the sudden turn on of space charge. The best suggestion, of course, is to turn on space charge adiabatically (increasing it in many turns). Then the bunch emittance must be conserved. However, this option is not available in ESME at the moment. Another method is to start with a smaller emittance and hope that the emittance would blowup to the desired value before transition after turning on space charge suddenly. This method is pretty difficult, because it is hard to know what emittance to start with.

Fortunately, the mismatch is not big. If we assume an rms bunch length of $\sigma_\phi =$

$\pi/9$ rf rad, for a 5-turn beam intensity of $N_0 = 1.8 \times 10^{10}$ per bunch, the maximum space-charge potential per turn is only

$$E_{sc} = e^2 h^2 \omega_0 \frac{gZ_0}{2\beta\gamma^2} \frac{N_0}{\sqrt{2\pi}} \frac{e^{-1/2}}{\sigma_\phi^2} = \begin{cases} 28.8 \text{ keV} & \text{at injection } \gamma = 9.5, \\ 7.45 \text{ keV} & \text{at transition } \gamma = 18.75, \end{cases} \quad (4.1)$$

where $h = 1113$ is the rf harmonic and $\omega_0/2\pi \sim 47.7$ kHz is the revolution frequency. A Gaussian bunch has been assumed. This amounts to only $\sim 3\%$ ($\sim 0.7\%$) of a 1 MV rf.

2. Incorrect binning

In ESME, after each turn, the voltage seen by a particle is computed by convoluting the bunch spectrum with the coupling impedance. To obtain the bunch spectrum, the rf wavelength is divided into N_b equal bins and a fast Fourier transform is performed. As is shown in Appendix A, the statistical rms error in the space-charge voltage is

$$\Delta E_{sc} = e^2 h^2 \omega_0 \frac{gZ_0}{2\beta\gamma^2} \frac{N_0}{2\pi\sqrt{6}} \sqrt{\frac{N_b^3}{N_t}}. \quad (4.2)$$

This ‘‘cubic rule’’ was first derived by Wei.⁵ It is clear that a small bin number N_b is crucial in reducing the error of computation. However, we do not want to sacrifice the high-frequency details of the simulations. With a beam pipe radius of 3.5 cm, we need at least 61.7 waves in a rf wavelength in order to cover up to the first propagating TM wave. In a fast Fourier transform of N_b bins, we can only obtain up to $N_b/2$ waves because the other $N_b/2$ higher frequency components are just a repetition of the lower frequency components. For this reason, the smallest number of bins used can only be $N_b = 128$. If we track $N_t = 5000$ macro-particles, the fractional error per turn is still 67%. Further increase in the number of macro-particles increases the computer time by very much. Nevertheless, as shown in Fig. 4(a) and (b), the fractional growth in bunch emittance before transition has drastically reduced to 1.1% with no particle loss.

In ESME, we can introduce space-charge MSC times per particle revolution by changing the input parameter MSC. This can also help in reducing the space-charge statistical error by a factor of $\sqrt{\text{MSC}}$ if the errors in successive applications of space charge are random. The analysis is given in Appendix B. We find that this is indeed

the case for a larger number of bins. For example, the tracking results with $N_b = 256$ and $MSC = 10$ are very similar to the results with $N_b = 128$ and $MSC = 1$. In both cases, $N_t = 5000$. However, changing MSC from 10 to 50 in the $N_b = 256$ case does not improve the result by very much. This is because the redistribution of particles in the bins is not big enough when the application of space-charge is too frequent, and the errors of successive applications are no longer random. This is especially true when the bin number is small. For example, with $N_b = 128$, the fractional growth of bunch emittance before transition is 0.3% when $N_t = 40000$ and $MSC = 1$. However, we see the a larger growth of 0.83% instead when $N_t = 5000$ and $MSC = 10$. The results of the latter simulation are shown in Fig. 5(a) and (b). For $N_t = 5000$ and $N_b = 128$, we find from Figs. 4 and 5 that the improvement in growth before transition is minimal when we increase MSC from 1 to 10. An analysis of the randomness of error is presented in Appendix C.

V. RESULTS OF SIMULATIONS WITH SPACE CHARGE

These simulations were all performed with $N_t = 5000$, $N_b = 128$, $MSC = 10$, and $\alpha_1^{\mathcal{P}} = 3.0 \times 10^{-3}$. We preferred $MSC = 10$ because this would lead to a smoother application of the space-charge force, although it would not help much in the reduction of statistical errors. The result for the change in bunch emittance through transition as a function of initial bunch emittance is shown in Figs. 6. Note that in the simulations with space charge, a different value of initial bunch emittance corresponds to a different intensity according to Table 1. Comparing Figs. 2(a) and 6, we can see the extra growth of bunch emittance due to space-charge mismatch, although the effect is not big. The data in Fig. 6 tend to have the $\sqrt{\epsilon_L}$ behavior, although different points correspond to different bunch intensities. We do not see any particle loss across transition because the largest initial bunch emittance was only $\epsilon_L = 0.16$ eV-sec corresponding to the 5-turn intensity. When space charge is turned off in Fig. 2(b), we also see no particle loss at and below this initial bunch emittance. We may conclude that microwave growth due to space charge was small in the simulations and the dominating mechanism is nonlinear effect.

A simulation was also performed with $\alpha_1^{\mathcal{I}} = -3/2$ or $\alpha_1^{\mathcal{P}} = -5.6 \times 10^{-3}$ and initial bunch emittance 0.16 eV-sec. This implies that the nonlinear time in Eq. (3.1) vanishes. The only contributions to transition crossing are space charge and higher-

order nonlinearity. The fractional growth across transition was found to be 6%. On the other hand, we see from Fig. 2(a) that the growth was 15.5% if space charge was turned off but $\alpha_1^{\mathcal{P}} = 3.0 \times 10^{-3}$ was retained. This gives another indication that nonlinearity dominates over space charge.

VI. COMPARISON WITH EXPERIMENT

The simulation results for emittance growth across transition agree in general with the values observed in reality.⁷ However, particle losses were observed at 2 turn when the initial emittance was larger than 0.11 eV-sec. The disagreement may arise from the fact that the effect of the MR impedance other than space charge had not been included in the simulations. The effective impedance per harmonic of the space charge at transition is about 3.5Ω according to Eq. (2.6). Although we do not know accurately the impedance per harmonic of the MR, we believe that it is at least 10Ω . Of course, in the actual performance of the MR, there can also be other contributions such as noises, mismatch, etc, which had not been included in the simulations. As a result, we do not consider the above disagreement between simulations and experimental measurements an actual discrepancy.

APPENDIX A. STATISTICAL ERROR DUE TO BINNING

At rf position ϕ , a particle receives an energy gain due to space charge per turn

$$E_{sc} = e^2 \hbar^2 \omega_0 \frac{g Z_0}{2\beta\gamma^2} \frac{\partial \lambda}{\partial \phi} \Big|_{\phi}, \quad (\text{A.1})$$

where λ is the linear number density of the bunch per unit rf radian. The rf wavelength is divided equally into N_b bins. Let n_i be the number of macro-particles in the i th bin at some turn. Then the bunch density there is

$$\lambda_i = \frac{n_i N_0}{\Delta\phi N_t}, \quad (\text{A.2})$$

where

$$\Delta\phi = \frac{2\pi}{N_b} \quad (\text{A.3})$$

is the bin size in rf radian. The last factor in Eq. (A.2) scales N_t , the number of macro-particles tracked, to N_0 , the actual number of particles in the bunch.

We first evaluate E_{sc} for particles in the i th bin in the time domain. Following essentially Ref. 5, we obtain

$$\frac{\partial \lambda}{\partial \phi} \Big|_i = \frac{n_i - n_{i-1}}{(\Delta\phi)^2} \frac{N_0}{N_t}. \quad (\text{A.4})$$

Since n_i is statistical and is usually much bigger than 1, the rms error (or square root of variance) is

$$\Delta \frac{\partial \lambda}{\partial \phi} \Big|_i = \frac{\sqrt{2} N_b^2 N_0}{4\pi^2 N_t} \sqrt{n_i} = \frac{\sqrt{2} N_0}{4\pi} \sqrt{\frac{N_b^3}{N_t}}. \quad (\text{A.5})$$

where Eq. (A.3) and $\langle n_i \rangle = N_t/N_b$ have been used. This error is therefore large at injection when $\gamma = 9.5$ and decreases by almost four times near transition where $\gamma = 18.75$.

For a Gaussian bunch the number density is

$$\lambda(\phi) = \frac{N_0}{\sqrt{2\pi}\sigma_\phi} e^{-\phi^2/2\sigma_\phi^2}, \quad (\text{A.6})$$

where σ_ϕ is the rms bunch length in rf radian. The maximum of the gradient of λ occurs at $\phi = \sigma_\phi$, giving

$$\frac{\partial \lambda}{\partial \phi} \Big|_{\max} = \frac{N_0 e^{-1/2}}{\sqrt{2\pi}\sigma_\phi^2}. \quad (\text{A.7})$$

Thus, the fractional error per turn is

$$\left. \frac{\partial \lambda}{\partial \phi} \right|_{\max} = 2\pi^{\frac{1}{2}} e^{\frac{1}{2}} \left(\frac{\sigma_\phi}{2\pi} \right)^2 \sqrt{\frac{N_b^3}{N_t}}. \quad (\text{A.8})$$

At injection $\sigma_\phi \approx \pi/7$ rf rad and gradually decreases to 0.082 rf rad at transition. The fractional error at transition therefore decreases to only $\sim 4.5\%$ of its value at injection.

A higher-order differentiation formula can be used instead of Eq. (A.4). For example, if we use

$$\begin{aligned} \left. \frac{\partial \lambda}{\partial \phi} \right|_i &= \frac{n_{i+1} - n_{i-1}}{2\Delta\phi}, \\ \left. \frac{\partial \lambda}{\partial \phi} \right|_i &= \frac{3n_i - 4n_{i-1} + n_{i-2}}{2\Delta\phi}, \\ \left. \frac{\partial \lambda}{\partial \phi} \right|_i &= \frac{-n_{i+2} + 4n_{i+1} - 3n_i}{2\Delta\phi}, \end{aligned} \quad (\text{A.9})$$

respectively, for the center, backward, and forward differences, the error will be reduced by a factor of 2 in Eqs. (A.5) and (A.8).

We next pursue the problem in the frequency domain. This is usually necessary if we want to incorporate impedances other than space charge. A fast Fourier transform leads to a density spectrum of

$$\tilde{\lambda}_m = \frac{1}{2\pi} \sum_{j=1}^{N_b} \left(\frac{n_j}{\Delta\phi} \right) \left(\frac{N_0}{N_t} \right) e^{im\phi_j} \Delta\phi. \quad (\text{A.10})$$

The voltage gained per turn by a particle in the i th bin is proportional to

$$\begin{aligned} v_i &= \frac{N_0}{2\pi N_t} \sum_{m=-N_b}^{N_b} im \sum_{j=1}^{N_b} n_j e^{im(\phi_j - \phi_i)} \\ &= -\frac{N_0}{2\pi N_t} \sum_{m=1}^{N_b} \sum_{j=1}^{N_b} n_j m \sin m(\phi_j - \phi_i), \end{aligned} \quad (\text{A.11})$$

which is in fact the same as $-\partial\lambda/\partial\phi$ of Eq. (A.4). The variance of v_i is

$$\text{Var}(v_i) = \frac{N_0^2}{4\pi^2 N_t^2} \sum_{m=1}^{N_b} \sum_{j=1}^{N_b} n_j m^2 \sin^2 m(\phi_j - \phi_i). \quad (\text{A.12})$$

The summation over m can be approximated by an integral to give

$$\sum_{m=1}^{N_b} m^2 \sin^2 m(\phi_j - \phi_i) = \frac{N_b^3}{6} \left[1 - \frac{3}{16\pi^2} \frac{1}{(i-j)^2} \right]. \quad (\text{A.13})$$

Since there is no $i=j$ term, $(i-j)$ varies from 1 to N_b-1 . The above sum is therefore $\sim N_b^3/6$, and

$$\text{Var}(v_i) = \frac{N_0^2}{24\pi^2} \frac{N_b^3}{N_t}. \quad (\text{A.14})$$

Finally, the fractional rms error is

$$\frac{\Delta v_i}{v_i} = \frac{\sigma_\phi^2 e^{\frac{1}{2}}}{\sqrt{12\pi}} \sqrt{\frac{N_b^3}{N_t}}, \quad (\text{A.15})$$

to be compared with Eq. (A.8). Note that the error in the frequency-domain computation is larger than the error in the direct time-domain computation, although both of them follow a ‘‘cubic rule.’’

APPENDIX B. PROBLEM OF MSC

If space charge is applied once per turn ($\text{MSC} = 1$), the rms error per turn is ΔE_{sc} given by Eqs. (A.1) and (A.5). If we set $\text{MSC} = M$, space charge is applied M times per turn in the amount of $1/M$ of E_{sc} at each application. The rms error for each application is therefore

$$\Delta E_{\text{sc}}^M = \frac{\Delta E_{\text{sc}}}{M}. \quad (\text{B.1})$$

If successive applications of space charge to particles in a bin were *random*, the total rms error per turn would accumulate to

$$\sqrt{M} \Delta E_{\text{sc}}^M = \frac{\Delta E_{\text{sc}}}{\sqrt{M}}, \quad (\text{B.2})$$

which is \sqrt{M} times smaller than when $M = 1$.

APPENDIX C. PROBLEM OF RANDOMNESS

A particle makes a synchrotron oscillation in $1/\nu_s$ turns. Therefore, between two successive applications of space charge ($\text{MSC} = M$ times per turn), the average rf angle through which the particle moves is given by

$$\delta\phi = \frac{2\sqrt{2\pi}\sigma_\phi\nu_s}{M}. \quad (\text{C.1})$$

In the above, we have assumed a bi-Gaussian distribution in the longitudinal phase space and all particles oscillate with the same synchrotron frequency. With N_b bins, number of macro-particles per bin in the *bunch region* is

$$n_b \approx \frac{\pi N_t}{\sigma_\phi N_b}. \quad (\text{C.2})$$

Outside the bunch region, number per bin is essentially zero. Thus, between two successive space-charge applications, the number of macro-particles moving out of or moving into a certain bin is

$$\delta n_b^\pm \approx \frac{n_b \delta \phi}{2\pi/N_b}, \quad (\text{C.3})$$

where $2\pi/N_b$ is the size of a bin in rf radian. Combining Eqs. (C.1) to (C.3), the total change of number of macro-particles in a bin is

$$\delta n_b = \delta n_b^+ + \delta n_b^- \approx \frac{2\sqrt{2\pi} N_t \nu_s}{M}, \quad (\text{C.4})$$

and the fractional change is

$$\frac{\delta n_b}{n_b} \approx \frac{4\sigma_\phi \nu_s N_b}{\sqrt{2\pi} M}. \quad (\text{C.5})$$

At the beginning of the MR cycle, the bunch is rather long, having $\sigma_\phi \sim \pi/7$. The synchrotron tune is also rather large, $\nu_s \sim 0.012$. Therefore, with $N_t = 5000$, the number of macro-particles moving into and out of a bin is

$$\delta n_b \sim \begin{cases} 301 & M = 1, \\ 30 & M = 10, \end{cases} \quad (\text{C.6})$$

independent of the number of bins. Of course, some of these particles that move out of the bin may not be inside the bin originally, but are transferred from neighboring bins. The percentage changes in particles per bin for bin number $N_b = 512, 256,$ and 128 are given in Table II. We see that for $N_b = 512$, the particles in each bin are changed completely for $M = 1$ and mostly for $M = 10$. Therefore, we expect the space-charge error to reduce by $\sqrt{10}$ when we vary MSC or M from 1 to 10. For $N_b = 256$, the particles are only partially altered with $M = 10$. Therefore, the reduction in error is less than $\sqrt{10}$. For $N_b = 128$, only 11% of the particles move into and out of the bin when $M = 10$. As a result, we see very little reduction in space-charge error in the simulation when M is increased from 1 to 10.

Although the fractional change is proportional to $\sigma_\phi \nu_s$, which decreases to zero at transition, as was pointed out in Appendix A, the fractional space-charge error decreases to only 4.5% of its value at injection. Therefore, it is sufficient to discuss the problem of randomness only near injection.

| MSC | $N_b = 512$ | $N_b = 256$ | $N_b = 128$ |
|-----|-------------|-------------|-------------|
| 1 | 440% | 220% | 110% |
| 10 | 44% | 22% | 11% |

Table II: Percentage particle change in a bin between two successive applications of space charge for different bin number N_b and MSC.

REFERENCES

1. S. Stahl and J. MacLachlan, Fermilab Report TM-1650, 1990.
2. K. Johnsen, *Effects on Nonlinearities on Phase Transition*, CERN, Symposium on High Energy Accelerators, Geneva, 1956, Vol. 1, p.106.
3. See for example, A. Sørensen, *Particle Accelerators* **6**, 141 (1975).
4. K.Y. Ng, *Some Estimation Concerning Crossing Transition of the Main Injector*, Fermilab Report TM-1670 (MI-30), 1990.
5. J. Wei, *Longitudinal Dynamics of the Non-Adiabatic Regime on Alternating-Gradient Synchrotrons*, Ph.D. thesis, State University of New York at Stony Brook, 1990.
6. J. Wei, *Transition Crossing in the Main Injector*, to be published in Proc. of the Fermilab III Instabilities Workshop, Fermilab, June 25-29, 1990.
7. I. Kourbanis, K. Meisner and K.Y. Ng, *Experimental Study of the Main Ring Transition Crossing*, Fermilab Report TM-1693, 1990.

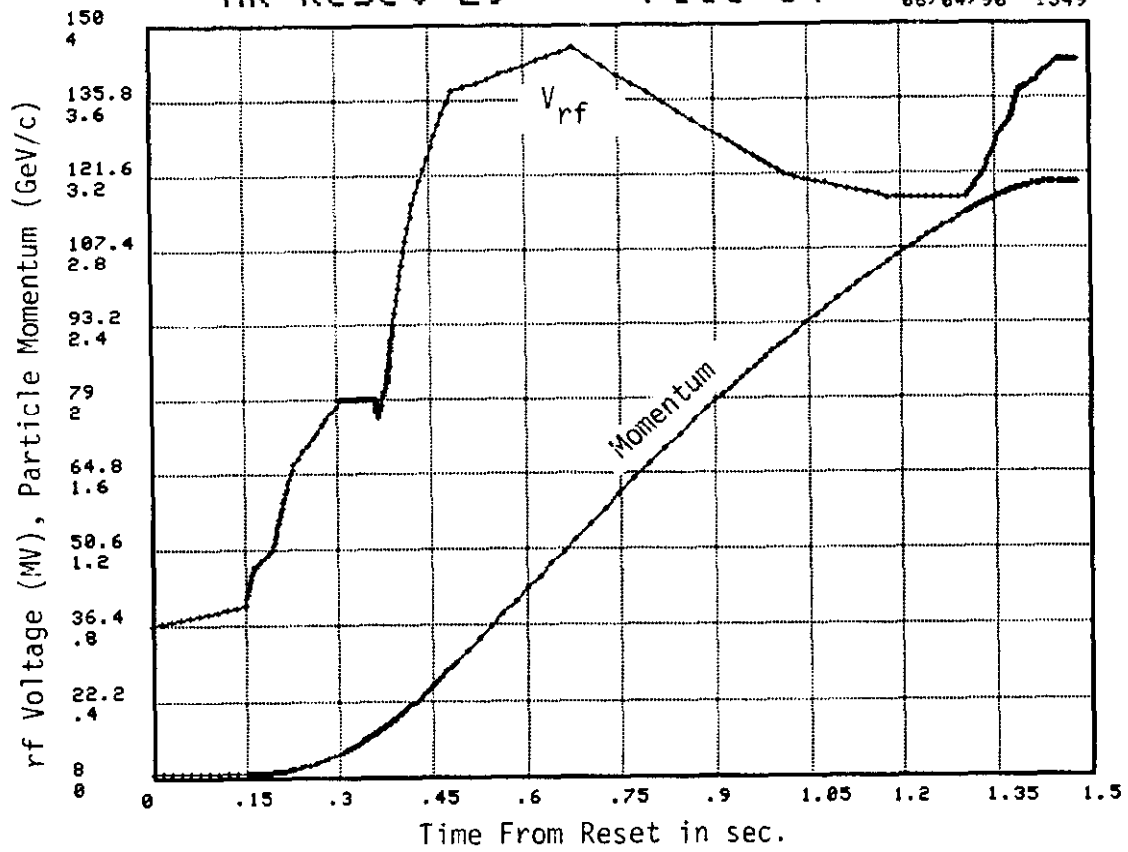


Fig. 1. RF Voltage and Momentum as a function of time in a 29-MR cycle.

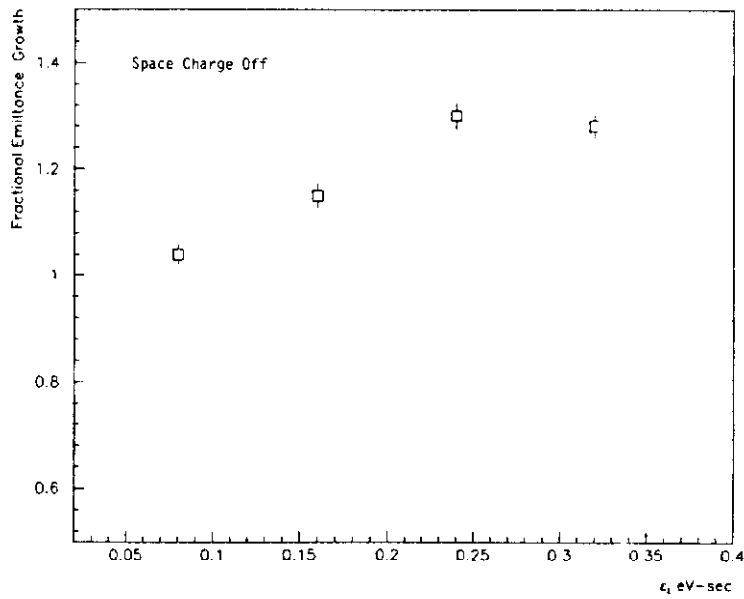


Fig. 2(a). Change in bunch area as a function of initial bunch emittance without space charge.

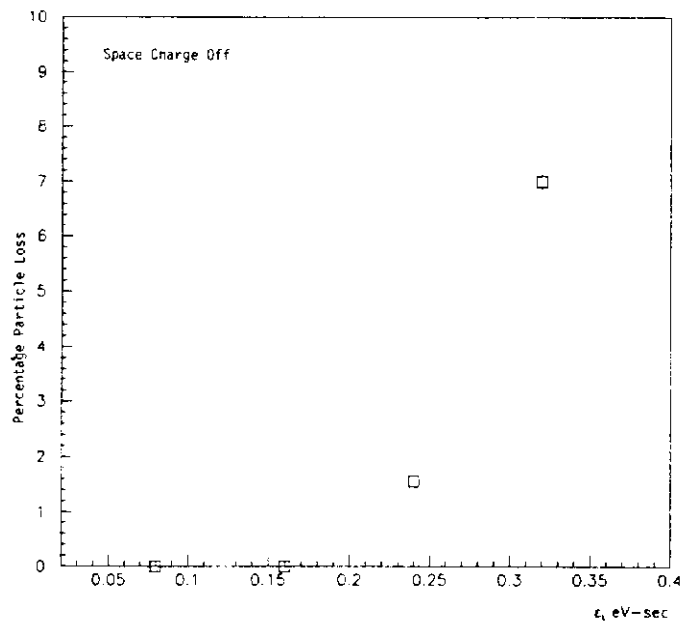


Fig. 2(b). Particle loss through transition versus initial bunch emittance without space charge.

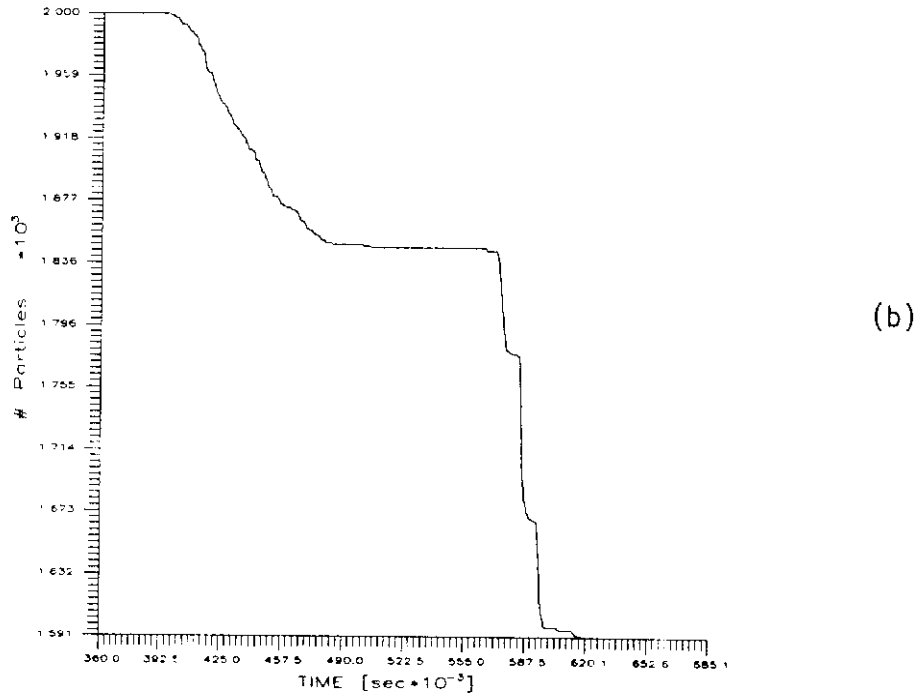
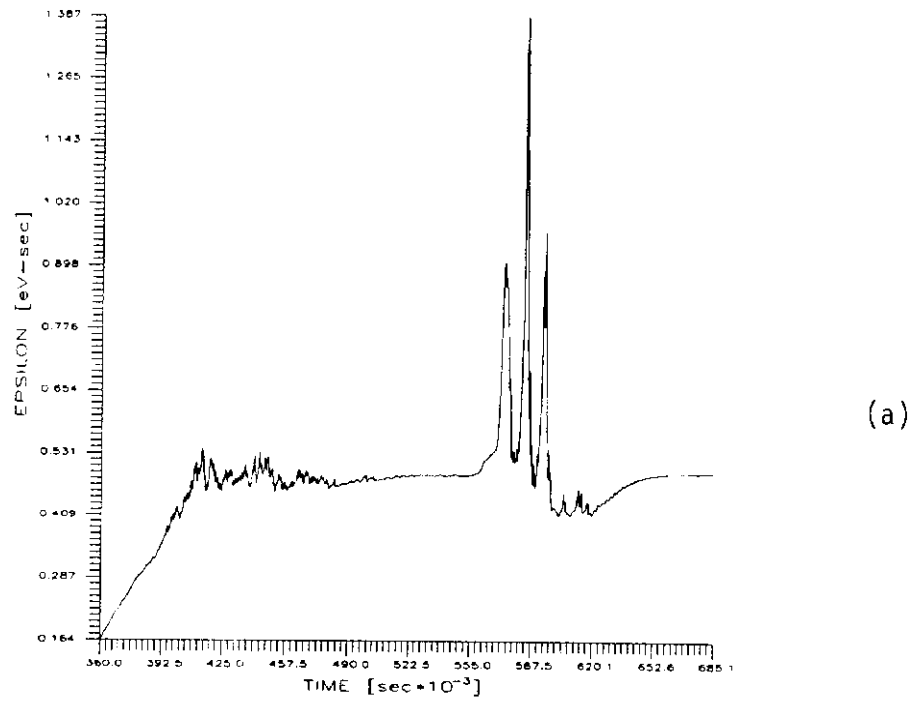
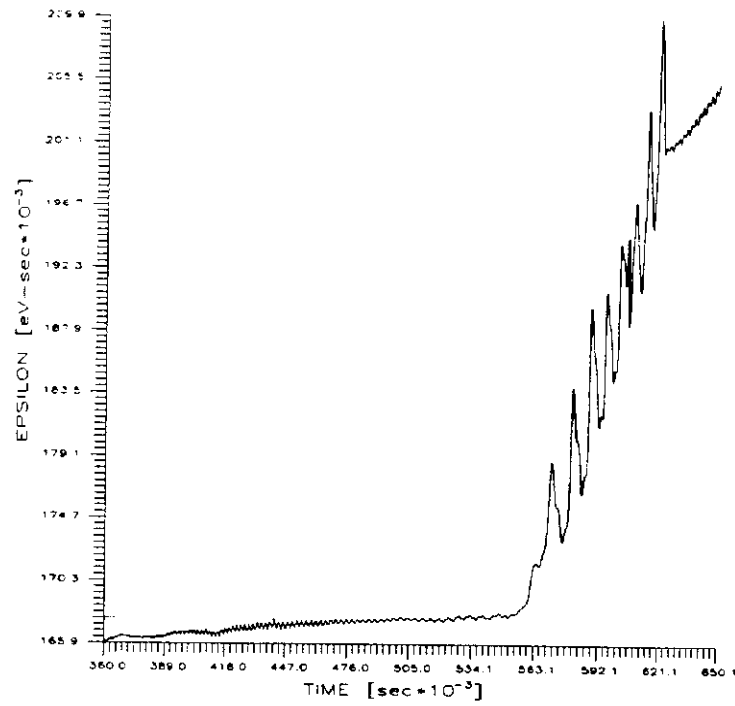
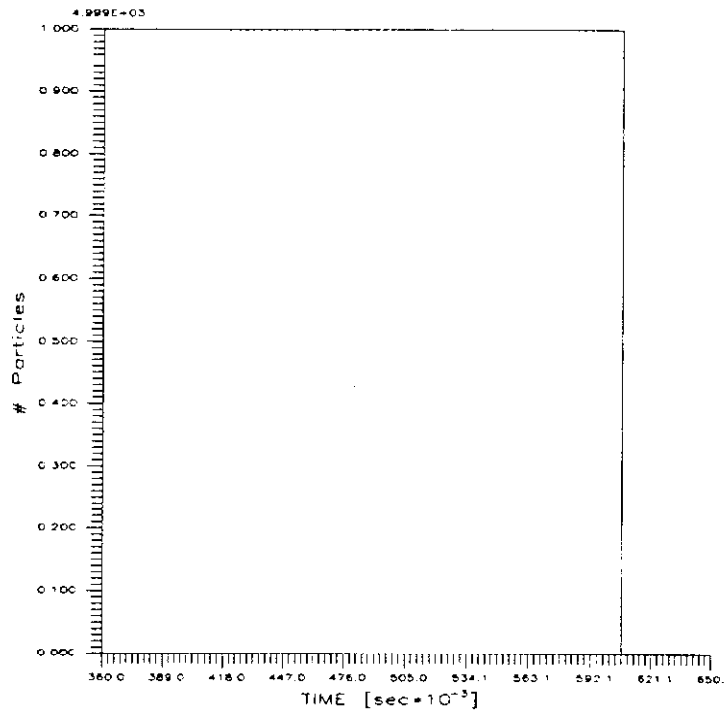


Fig. 3. Simulation with space charge for 5-booster turns with $N_t = 2000$, $N_b = 512$, $MSC = 1$, $\alpha_t^E = 1.0 \times 10^{-3}$. (a) Longitudinal emittance versus time. (b) Percentage particle loss versus time.

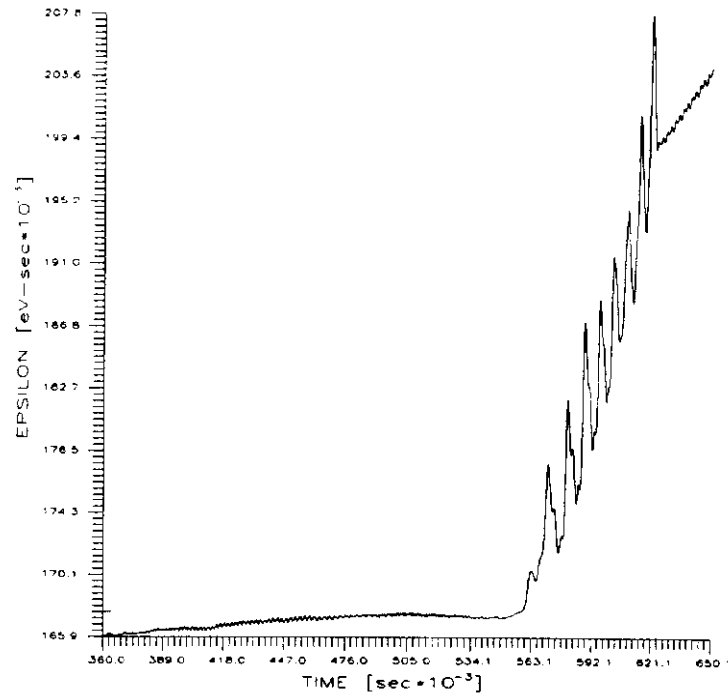


(a)

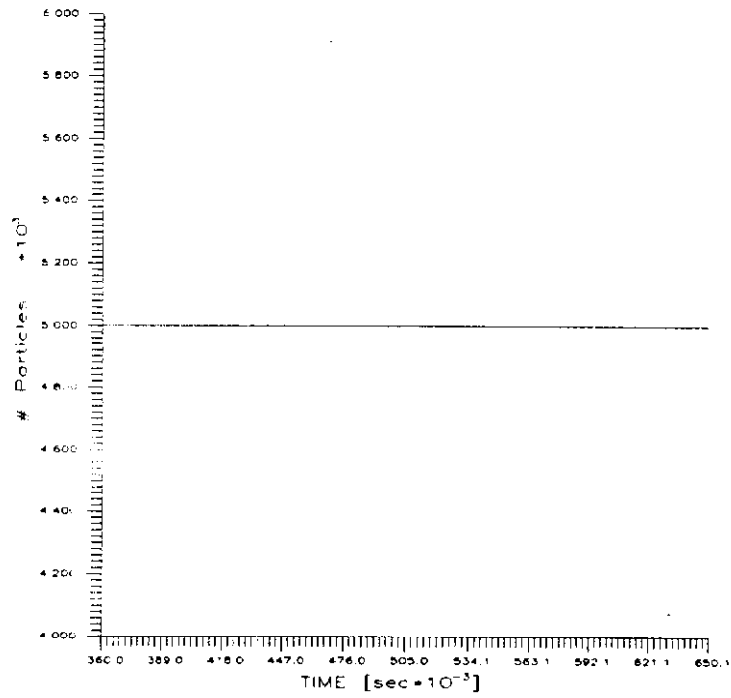


(b)

Fig. 4. Simulation with space charge for 5-booster turns with $N_t = 5000$, $N_b = 128$, $MSC = 1$, $\alpha_1^E = 3.0 \times 10^{-3}$. (a) Longitudinal emittance versus time. (b) Percentage particle loss versus time.



(a)



(b)

Fig. 5. Simulation with space charge for 5-booster turns with $N_t = 5000$, $N_b = 128$, $MSC = 10$, $\alpha_1^E = 3.0 \times 10^{-3}$. (a) Longitudinal emittance versus time.
 (b) Percentage particle loss versus time.

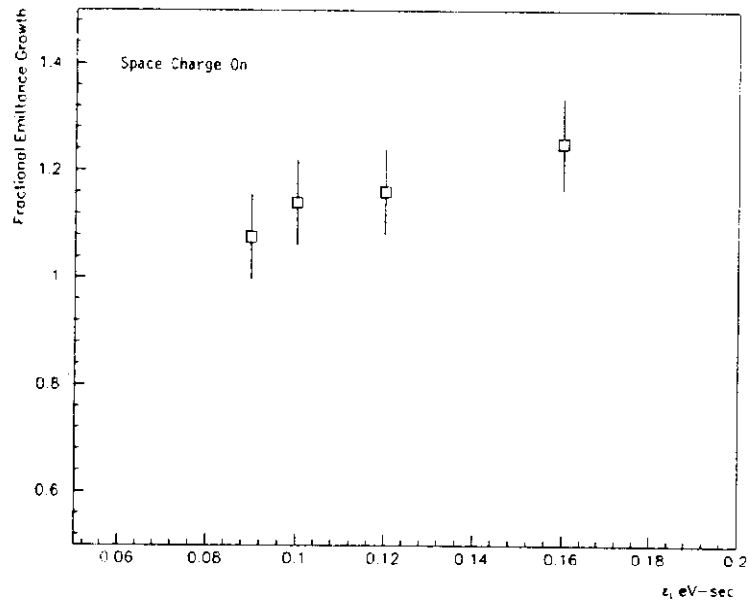


Fig. 6. Change in bunch area as a function of initial bunch emittance with space charge.